Available online at www.sciencedirect.com

ScienceDirect

Energy Procedia 71 (2015) 320 – 327

Energy Procedia

The Fourth International Symposium on Innovative Nuclear Energy Systems, INES-4

Effect of annealing on thermal diffusivity in ceramics irradiated by electrons and neutrons

Masafumi Akiyoshi[a] *, Ikuji Takagi[b], Toshimasa Yoshiie[c], Xu Qiu[c], Koichi Sato[c], Toyohiko Yano[d]

[a] *Department of Nuclear Engineering, Kyoto University, Kyoutodaigaku-Katsura, Nishikyou-ku, Kyoto 615-8540, Japan*
[b] *Quantum Science and Engineering Center, Kyoto University, Uji, Kyoto 611-0011, Japan*
[c] *Research Reactor Institute, Kyoto University, Kumatori-cho, Osaka 590-0494, Japan*
[d] *Research Laboratory for Nuclear Reactors, Tokyo Institute of Technology, 2-12-1 Ookayama, Meguro-ku, Tokyo 152-8550, Japan*

Abstract

α-Al_2O_3, AlN, β-Si_3N_4, and β-SiC ceramic specimens were irradiated by a 30 MeV electron beam up to 0.01 dpa at 80 ℃, and they started to recover thermal diffusivity with annealing from 300–500 ℃. In previous studies, similar ceramics were heavily neutron-irradiated in a fast reactor, JOYO, and the neutron-irradiated β-Si_3N_4 and β-SiC also showed recovery above 400 ℃, though they were irradiated at 502 ℃ or 738 ℃. This result is explained by the hypothesis that a 'primary' irradiation occurred at the set temperature, and after that, a 'secondary' irradiation occurred at a lower temperature during the shutdown process of the reactor. In contrast, the neutron-irradiated α-Al_2O_3 and AlN did not show such unexpected recovery, but showed recovery above 800-900 ℃. This difference is explained on the basis of structural models of dislocation loops namely, the 'pileup' model and the 'nano-partition' model.

Selection and peer-review under responsibility of the Tokyo Institute of Technology

Keywords: ceramics; neutron irradiation; electron irradiation; thermal diffusivity; isochronal annealing

1. Introduction

Thermal diffusivity is one of the most important characteristics of ceramic materials used in fusion reactors. In ceramics, unlike metals, heat is mainly carried by phonons. Phonon transportation is obstructed by lattice defects, especially vacancies. It has been reported that neutron-irradiated specimens show severe degradation in thermal diffusivity because of irradiation induced defects [1,2].

In previous studies [1,3,4], thermal diffusivity or conductivity during irradiation was estimated from post-irradiation measurements using several assumptions. One assumption is that the amount of 'transient defect' during irradiation is small enough . Here, 'transient defect' is considered that it exists for a very short time during irradiation. Dynamic effects due to 'transient defects' during irradiation are an important issue to understand the processes that produce defects [5,6]. However, only a few in-situ experimental studies have been conducted [1,7,8] except investigations of electron excitation like radiation induced conductivity (RIC) [9–11] or luminescence measurements [12,13]. Hence, an in-situ measurement of positron annihilation lifetime (PAL) during ion-beam irradiation is now on early practice [1,7], and the results validate the assumption to a large extent.

However, another assumption is required to enable the estimation mentioned above, that is, the irradiation temperature is constant. That means that in a test irradiation environment, the temperature is kept constant during irradiation, while a material used in a real-life fusion reactor encounters a constant heat load. Specimens that are neutron-irradiated heavily contain many types of defect, such as interstitial atoms, vacancies, dislocation loops, voids, and so on. These defects interact with each other and their amount and size are changed

*Phone/Fax : +81-75-753-4837, e-mail: akiyoshi@nucleng.kyoto-u.ac.jp

Selection and peer-review under responsibility of the Tokyo Institute of Technology
doi:10.1016/j.egypro.2014.11.885

during irradiation at elevated temperature. Irradiation temperature changes the reaction velocity, accordingly it changes the distribution of defects. Then the modified distribution of defects changes thermal diffusivity of the specimen. Under a constant heat flux environment, the temperature of a specimen is determined by its thermal diffusivity. Therefore, these correlations make it difficult to fix the temperature of the specimen during irradiation.

To resolve this problem, an analysis based on reaction kinetics is required. In this analysis, the reaction between interstitial atoms, vacancies, dislocation loops, and voids is explained by their density and reaction velocity. In the simplest model, the correlation is described as below.

- $\mathrm{I} + \mathrm{I}_n \rightarrow \mathrm{I}_{n+1}$
- $\mathrm{I} + \mathrm{V} \rightarrow 0$
- $\mathrm{V} + \mathrm{V}_n \rightarrow \mathrm{V}_{n+1}$

where I: interstitial atom, I_n: cluster of interstitial atoms that contains n atoms, V: vacancy, V_n: cluster of vacancies that contains n vacancies, and 0 represent no defect. In ceramics, a cluster of interstitial atoms is usually an interstitial dislocation loop, and a cluster of vacancies is usually a void. During neutron irradiation, these reactions conflict each other, so it is difficult to determine the velocity of each reaction. In previous studies, specimens that were neutron-irradiated heavily were annealed to study their recovery behavior [1, 14–18]. The recovery of thermal diffusivity was compared to that of macroscopic swelling and it partly represented the distribution of these defects. However, the discussions were qualitative and not quantitative.

On the other hand, electron irradiation induces a simple Frenkel pair. In this study, 30 MeV electron accelerator KURRI(Kyoto University Research Reactor Institute)-Linac was used to induce point-defects in bulk ceramic specimens and recovery behavior with annealing was compared to that of the heavily neutron-irradiated specimens.

The maximum energy of a primary knock-on atom (PKA) during the 30 MeV electron irradiation is obtained as $E_{\mathrm{p.max}} = 2E(E + 2m_0c^2)/Mc^2$ where $E_{\mathrm{p.max}}$: maximum PKA energy, E: incident energy of electron, m_0: rest mass of an electron, c: velocity of light and M: mass of a target. When the mass target is 16 amu, $E_{\mathrm{p.max}}$ is calculated as 125 keV. However, the average PKA energy was only 225 eV even by 30 MeV incident electrons, and the Kinchin-Pease model gives a displacement damage function as 3.75. This result shows that even using the 30 MeV electron irradiation, induced defects are mostly point defects like the Frenkel pair. Furthermore, the electron-irradiation in this study was performed at 80 ℃ in cooling water.

The neutron irradiation was performed up to several tens dpa above 500 ℃, and many interstitial dislocation loops were observed by transmission electron microscopy (TEM) [15, 17, 17–19]. This different defect distribution leads to different behavior with annealing.

2. Experimental

In this study, α-Al_2O_3, AlN, β-Si_3N_4 and β-SiC were selected as typical ceramic materials. It is well known that β-SiC is the most important material for nuclear applications, and α-Al_2O_3 is used as an insulator. In addition, AlN was selected because of its high thermal diffusivity before irradiation, which makes it easy to estimate the effect of induced defects. β-Si_3N_4 showed higher thermal diffusivity and lower swelling than β-SiC after high neutron irradiations [20], and this makes β-Si_3N_4 a candidate material for nuclear applications. Properties of the non-irradiated specimens used for electron-irradiation are listed in Table 1. The specimens used for neutron-irradiation were different from specimens used for electron-irradiation, and they were reported in detail in a previous work [1].

Electron irradiation on ceramic specimens was performed using the 30 MeV electron Linac at the Kyoto University Research Reactor Institute. The irradiation was operated in pulse mode with a peak current of 400 mA for 4 μs, and the frequency was 70-80 Hz, so beam current averaged about 110-140 μA in 2 cm^2. The range of the 30 MeV electron beam in ceramics is deeper than 5 cm, so the defects were induced equally allover the ϕ 10 mm×0.5 mm specimen with a dose of 1.0×10^{-2} dpa. Specimens were irradiated in flowing cold water in an aluminum chamber and irradiation temperature was kept at about 80 ℃.

The neutron irradiations were performed in the Japanese experimental fast reactor JOYO, and capsules of the specimens were enclosed in the Core Material Irradiation Rigs, CMIR-4. In the rigs, irradiation temperature of a specimen was determined by gamma heating of the specimen, sodium flow in the compartment, and heat conduction of the double-walled tubes. After the irradiation, the irradiation temperature of each capsule was confirmed using a Thermal Expansion Difference temperature (TED) monitor. Each capsule contained α-Al_2O_3, AlN, β-Si_3N_4 and β-SiC specimens, and they were irradiated under the same condition. The capsule

T51 was irradiated to 28 dpa (2.8×10^{26} n/m^2) at 502 ℃ and the capsule T57 was irradiated to 37 dpa (3.7×10^{26} n/m^2) at 738 ℃. The dimensions of these specimens were ϕ 3 mm×0.5 mm.

In this study, the thermal diffusivity was measured by a laser flash method using a custom-made measurement system (ULVAC Techno, TC-7000/Special) that can measure a ϕ 3 mm small disk, and results were analyzed using a conventional $t_{1/2}$ method. The laser power of each flash was 6 J in 1 ms and that increased the temperature of the specimen by about 10 ℃ with $t_{1/2} < 10$ms. The precision of thermal diffusivity with this measurement system is ±10% for a specimen of ϕ 3 mm or ±5% for ϕ 10 mm sample. All specimens were coated with a carbon spray and baked on a hot plate at 100 ℃ to avoid transmission of the laser flash. All measurements were performed at room temperature, and obtained thermal diffusivity was adjusted to that at 27 ℃ using the function $\alpha_{300} = \alpha_T T/300$, where α_{300} represents the thermal diffusivity at 27 ℃ (300 K), T is the measurement temperature and α_T is the measured thermal diffusivity at the temperature T. This adjustment assumes that thermal diffusivity, α, changes with temperature T as $\alpha = k/T$, where k is a constant. After the irradiation, a constant n, that represents the distribution of defects is added, and the temperature dependence was changed to $\alpha = k/T^n$ [3]. Nevertheless, the difference of the measurement temperature from 27 ℃ was small, so the simple function without the n parameter was used for the adjustment.

After the measurement on the as-irradiated specimens, isochronal annealing was conducted every 100 ℃ up to 1100 ℃ for electron-irradiated specimens or 1400 ℃ for neutron-irradiated specimens in vacuum. Specimens were annealed for 1 h at a set temperature. After the annealing, specimens were cooled in the furnace to room temperature and thermal diffusivity measurements were performed. Annealing above 1200 ℃ was not carried out for the electron-irradiated specimens to avoid contamination with radio active nuclides created by transmutation such as ^{3}H or ^{14}C. The annealing and measurement of the electron-irradiated specimens was performed at the Radiation Laboratory in the Uji-Campus of Kyoto University.

Table 1 Properties of ceramic specimens for electron irradiation

material	α-Al_2O_3	AlN	β-Si_3N_4	β-SiC
manufacturer	Toray	Tokuyama	Toray	Bridgestone
product name	A-999	SH-30	SN	PB-S
sintering method	pressureless	pressureless	hot-press	hot-press
thermal diffusivity [10^{-4} m^2/s]	0.12	0.74	0.11	1.1
density [10^3 kg/m^3]	3.9	3.34	3.2	3.15
Young's modules [GPa]	380	322	290	390
thermal conductivity [W/m·K]	38	174	25	230
volume resistivity [Ω·cm]	$> 10^{14}$	8.4×10^{13}	$> 10^{14}$	2.0×10^{-2}

3. Results

Figs. 1-(a)-1-(d) show recovery behavior of thermal diffusivity with isochronal annealing in the electron- and neutron-irradiated ceramic specimens. The error bar shows the standard deviation of the values measured about 10 times. In our earlier studies [14–18], the thermal diffusivity in the neutron-irradiated specimens was not corrected properly for the form factor (T51 and T57 neutron-irradiated specimens were ϕ 3 mm unlike a standard specimen that is ϕ 10 mm), so the evaluated values were a little different from the values obtained here.

All the electron-irradiated specimens showed recovery in thermal diffusivity from 300-500 ℃, even though the irradiation temperature was about 80 ℃. α-Al_2O_3, AlN, and β-Si_3N_4 specimens recovered linearly with annealing temperature. In the case of α-Al_2O_3 and β-Si_3N_4, the amount of degradation was small because their thermal diffusivity was low before irradiation (0.12 and 0.11×10^{-4} m^2/s). The electron-irradiated β-Si_3N_4 specimen (Fig.1-(c)) showed a little complex recovery, but it is indicated with a simple line because the precision was not fine enough to separate it to several stages. In addition, the eye-guide line uprose from a little lower temperature than the other specimens, but it is not sure with this single result. The electron-irradiated β-SiC specimen (Fig.1-(d)) also showed recovery from 300 ℃, but it did not recover linearly with the annealing temperature. In Fig.1-(d), eye-guide was drawn as a quadratic function of the annealing temperature, but the physical explanation for this behavior is not clear.

On the other hand, the neutron-irradiated specimens showed a complex recovery behavior. Thermal diffusivity of the neutron-irradiated α-Al_2O_3 recovered from 800-900 ℃ and follow a quadratic curve and then recovered gently above 1100–1200 ℃. The neutron-irradiated AlN showed a gradual recovery from 900 ℃, and then recovered rapidly above 1100–1200 ℃ as a quadratic function, but still had 70% degradation after annealing at 1500 ℃. The neutron-irradiated β-Si_3N_4 and β-SiC showed a small recovery from 400 ℃, that almost

corresponds to the case of the electron-irradiated specimen, but this temperature was lower than the neutron irradiation temperature. Subsequently, the neutron-irradiated β-Si_3N_4 and β-SiC recovered rapidly following quadratic curve above 1000 ℃ . The electron-irradiated β-SiC showed almost the same recovery curve, but the rapid recovery above 1000 ℃ is not confirmed. Further work may clarify this recovery behavior above 1000 ℃ in electron-irradiated specimens using an advanced annealing system that can enclose the radio-active nuclide safely.

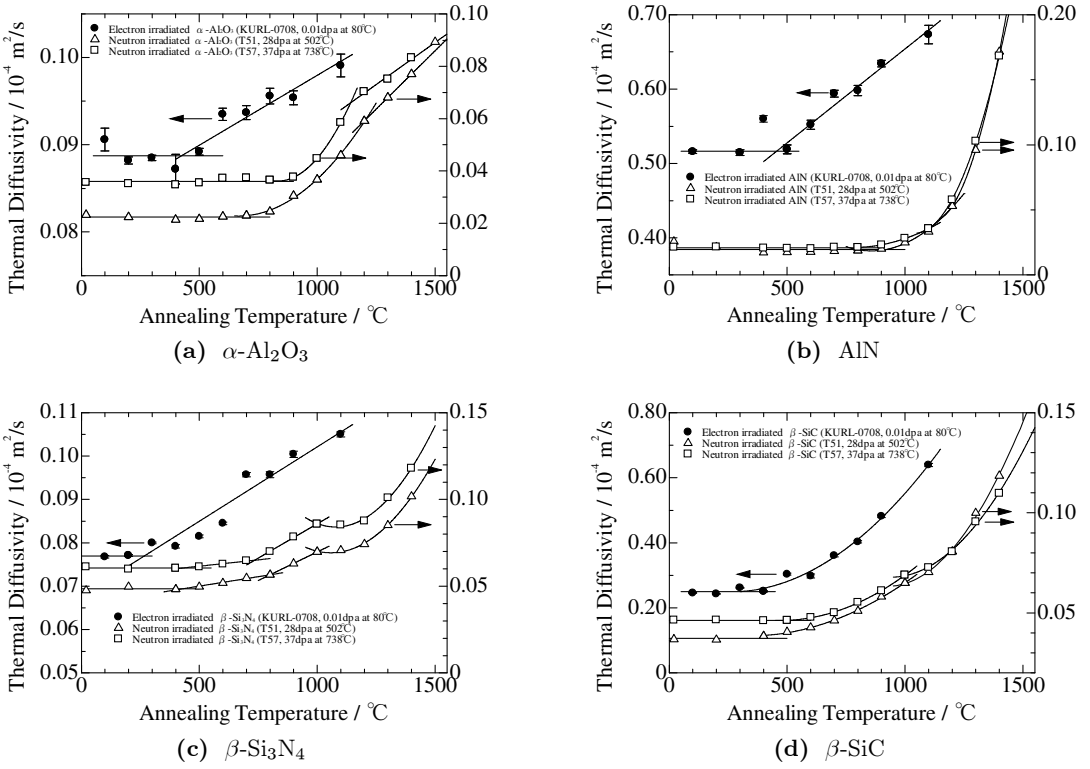

Fig. 1 Recovery behavior of thermal diffusivity in electron-irradiated ceramics with isochronal annealing. The filled symbols represent the electron-irradiated specimen shown with left-side axis, and the open symbols represent the neutron-irradiated specimen shown with right-side axis. (a) α-Al_2O_3 , (b) AlN, (c) β-Si_3N_4 and (d) β-SiC

4. Discussion

4.1 Recovery behavior of α-Al_2O_3 and AlN

In the case of the electron-irradiated α-Al_2O_3 and AlN specimens, thermal diffusivity recovered from 400 ℃, while the neutron-irradiated α-Al_2O_3 and AlN showed recovery above 800–900 ℃.

Earlier studies of annealing showed that the recovery of swelling in α-Al_2O_3 that was neutron-irradiated at 100 ℃ started below 200 ℃ [21], but on the other hand, α-Al_2O_3 that was neutron-irradiated at 200 ℃ recovered thermal diffusivity from 800 ℃ [22]. This difference is explained by the different distribution of defects, i.e., point defects or interstitial dislocation loops. It was reported that α-Al_2O_3 specimens neutron-irradiated at 150 ℃ showed the same amount of lattice parameter change between the a-axis and the c-axis, while specimens irradiated at 650 ℃ showed difference [23, 24]. This difference represents the amount of interstitial dislocation loops. This difference become larger as the irradiation temperature rose and showed a small difference even at 400 ℃ [25, 26].

It was also reported that AlN neutron-irradiated at 100 ℃ showed recovery from 100 ℃ both in swelling and thermal diffusivity [27, 28]. AlN specimens neutron-irradiated at 470 ℃ showed a difference between the lattice parameter of the a-axis and the c-axis, and these lattice parameters and the macroscopic length were recovered starting from 900 ℃. In another specimen neutron-irradiated at 100 ℃ , the lattice parameter change in the a-axis and the c-axis and the change in the macroscopic length were same, and they recovered from 100 ℃ [29].

These studies showed that in the case of α-Al_2O_3 and AlN, interstitial atoms obtained enough mobility to migrate and recombine with vacancies at 100 ℃, and clustered to form interstitial dislocation loops above 200 ℃, while recombination of vacancies and interstitial dislocation loops was restricted until 800 ℃. However, the electron-irradiated α-Al_2O_3 and AlN specimens showed recovery above 400 ℃, which is different from the behavior of neutron-irradiated specimens mentioned above. It is hypothesized that distribution of defects may be different between the electron-irradiated specimens and the neutron-irradiated specimens.

Fast neutron irradiation induces cascade defects, unlike electron irradiation. At the center of a cascade, many vacancies are induced in a small area, while interstitial atoms are dispersed at the periphery of the cascade. On the other hand, electron irradiation induces simple point defects. However, this difference in the distribution of defects does not explain the different recovery, because simple point defects recover more easily than cascade defects. Further study of the annealing behavior of electron-irradiated specimens is required to explain this.

4.2 Recovery behavior of β-Si_3N_4 and β-SiC

The neutron-irradiated β-Si_3N_4 and β-SiC showed a small recovery above 400 ℃. Several studies showed that neutron irradiation above 400 ℃ induced interstitial dislocation loops in SiC [2, 17] and in β-Si_3N_4 [15]. It was reported that SiC specimens neutron-irradiated at 470 ℃ showed a difference between the macroscopic swelling and the change in the lattice parameter measured by X-ray diffraction (XRD), while other specimens neutron-irradiated at 370 ℃ up to 15 dpa showed almost no difference [17, 30, 31]. Swelling in these specimens was recovered with annealing above the irradiation temperature. Even in an SiC specimen neutron-irradiated at 280 ℃, this recovery above the irradiation temperature was reported [32].

In this study, electron irradiation was performed at 80 ℃ and the recovery of thermal diffusivity in β-Si_3N_4 and β-SiC started around 300 ℃. This onset temperature is a little higher than the irradiation temperature. The annealing study of thermal diffusivity in β-Si_3N_4 and β-SiC is still not enough, and the lowest temperature to recover thermal diffusivity is not clear, unlike α-Al_2O_3 and AlN.

However, the neutron irradiation was performed at 502 ℃ or 738 ℃. Usually, recovery with annealing is observed above the irradiation temperature. In particular, SiC was used as a monitor for the irradiation temperature since the recovery of swelling was started from the irradiation temperature [33]. Hence, recovery of the irradiated specimens below the irradiation temperature is unexpected.

4.3 Defect structure model

The difference between the neutron-irradiated α-Al_2O_3, AlN, and β-Si_3N_4, β-SiC may arise from the difference in the crystal structure as discussed in a previous work [34], where the defect structure was explained by the 'pileup' model shown in Fig. 2 (α-Al_2O_3 and AlN) and the 'nano-partition' model shown in Fig. 3 (β-Si_3N_4 and β-SiC). In the pileup model, interstitial dislocation loops are inserted in the same hexagonal basal plane (0001) without any restriction on inducing a new loop. These interstitial dislocation loops work as sinks of interstitial atoms, so the concentration of interstitial atoms may be low. In the nano-partition model, interstitial dislocation loops are induced into crystallographically equivalent planes of forms they cross each other, while the crystal structure does not allow intersection, so this structure restricted the growth of loops or induction of new loops. Consequently, interstitial atoms lose sinks, and it may leave a higher concentration of interstitial atoms than in the case of the pileup model. This is explained differently using the 'BIAS effect' that is, the activation energy required to gather an interstitial atom to an interstitial dislocation loop is smaller than that required to recombine an interstitial atom with a vacancy, and dislocation loops work stronger as a sink of interstitial atoms than vacancies [35]. In α-Al_2O_3 and AlN, the BIAS effect is stronger than for β-Si_3N_4 and β-SiC at higher temperatures. In the case of electron irradiation, only point defects were induced in the both structure, so no BIAS effect was observed.

This model explains no recovery of thermal diffusivity in α-Al_2O_3 and AlN until 800 ℃ by hypothesizing that most interstitial atoms were captured into loops because of the strong BIAS effect, and few isolated interstitial atoms and many vacancies were left in the post-irradiated specimens. At a temperature higher than 800 ℃, it is believed that vacancies obtain enough mobility to migrate and then recombine with interstitial loops.

4.4 A hypothesis: 'secondary' irradiation at low temperature

However, the recovery below the irradiation temperature in the neutron-irradiated β-Si_3N_4 and β-SiC is not elucidated by the above explanation. This result could be because these specimens were irradiated at two different conditions. In other words, it is hypothesized that the specimens were irradiated once at the set temperature, and after that, they were exposed to a 'secondary' irradiation at lower temperatures while the reactor was shutting down. The specimens in this work were irradiated in the Core Material Irradiation Rig,

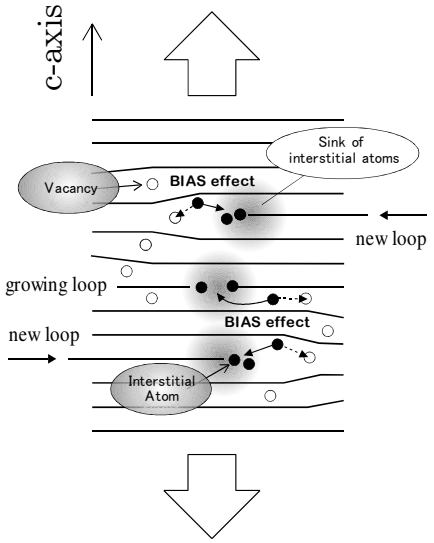

Fig. 2 Structure image model of 'pileup' dislocation loops on the (0001) plane.

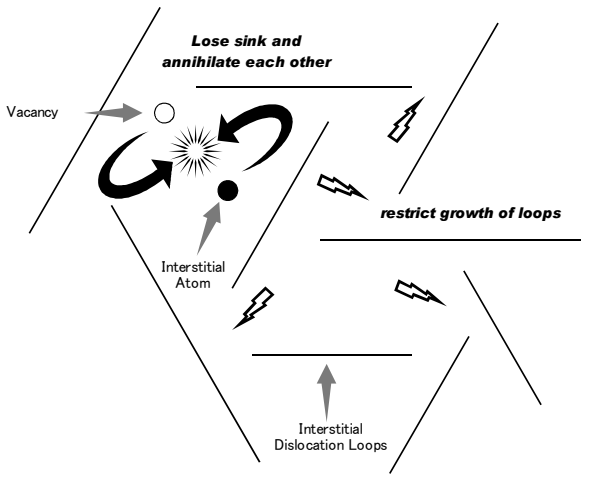

Fig. 3 Schematic model of 'nano-partitions' (dislocation loops which restrict to growth each other).

CMIR-4, that was loaded in the reactor-core with other fuel assemblies, so the samples were not removed until the irradiation cycle was finished. The neutron irradiation was performed in JOYO that have a high neutron flux of 5×10^{19} n/m^2·s near the core that gives 0.1 dpa within 6 h. During the shutdown process, the neutron flux was decreased by the control rod, but the flux did not decrease simply with the thermal power, so it is believed that the specimens were irradiated to a certain extent as mentioned above. Irradiation temperature in the CMIR was controlled by flux of molten-sodium coolant and γ-heating, but not controlled by any heater unlike MARICO (Material Testing Rig with Temperature Control) in JOYO. Snead et al. showed that an irradiation on SiC up to 0.1 dpa at 200 ℃ induced a larger swelling and thermal diffusivity degradation than that induced by an irradiation up to 10 dpa at 600 ℃ [2]. This investigation shows that the neutron-irradiated β-SiC contained considerable point defects induced by the 'secondary' irradiation at the lower temperature.

This 'secondary' irradiation also occurred on the α-Al_2O_3 and AlN specimens, but the recovery at low temperatures was not observed. In the case of β-SiC, degradation in thermal diffusivity leveled off at a relatively low dose (0.1-0.5 dpa at 480-550 ℃) [2], but on the other hand, α-Al_2O_3 showed further degradation until 10 dpa [36]. The heavily neutron-irradiated α-Al_2O_3 and AlN showed lower thermal diffusivity than β-Si_3N_4 and β-SiC. This is also explained by the BIAS effect. In the pileup structure, most interstitial atoms migrated and gathered to interstitial dislocation loops with a strong BIAS effect during the neutron irradiation performed at the set temperature, and the vacancies induced with these interstitial atoms were not affected. A higher concentration of these vacancies made the recombination probability of interstitial atoms induced by the 'secondary' irradiation higher than in the case of the nano-partition structure, where the BIAS effect was restricted and concentration of vacancies was low. Furthermore, additional degradation of thermal diffusivity induced by the 'secondary' irradiation was relatively low because of the higher concentration of vacancies during 'primary' irradiation. Thermal diffusivity, α, is obtained by $\alpha = \frac{1}{3}\mu\lambda$, where μ: mean speed of phonon and λ: mean free path of phonons, and the mean free path of phonons after irradiation (λ_I) is given as $1/\lambda_I = 1/\lambda_0 + 1/\lambda_{d1} + 1/\lambda_{d2}$ where λ_0 is for unirradiated material, λ_{d1} is related to the defects induced by the 'primary' irradiation, and λ_{d2} is related to the defects induced by the 'secondary' irradiation. In the case of the neutron-irradiated α-Al_2O_3 and AlN, λ_{d1} might be smaller than for the β-Si_3N_4 and β-SiC, so even if the same amount of vacancies are induced by the 'secondary' irradiation, it had a smaller contribution to thermal diffusivity after the irradiation.

5. Conclusion

α-Al_2O_3, AlN, β-Si_3N_4, and β-SiC ceramic specimens were irradiated by 30 MeV electron up to 0.01 dpa. All the electron-irradiated specimens started recovering thermal diffusivity with annealing from 300–500 ℃. In addition, neutron-irradiated β-Si_3N_4 and β-SiC showed recovery above 400 ℃. The electron irradiation was performed at 80 ℃, while the neutron irradiation was performed at 502 ℃ or 738 ℃. This recovery below the

irradiation temperature is unexpected. It is hypothesized that this is because 'primary' irradiation occurred at the desired temperature, and after that, a 'secondary' irradiation occurred at a lower temperature during the shutdown process of the reactor.

On the other hand, the neutron-irradiated α-Al_2O_3 and AlN did not show this unexpected recovery, but showed recovery above 800-900 ℃. This difference was explained by the structural model of dislocation loops. In the 'pileup' model, BIAS effect was strong and many vacancies were unaffected during the 'primary' irradiation. This made the contribution of the 'secondary' irradiation relatively low, because most of the interstitial atoms induced by the 'secondary' irradiation recombined with vacancies induced by the 'primary' irradiation. In contrast, in the 'nano-partition' model, interstitial atoms lose sink and the BIAS effect was restricted, so the density of vacancies was not so high during the 'primary' irradiation. Here, the 'secondary' irradiation at the lower temperature left a significant amount of interstitial atoms.

The electron-irradiated α-Al_2O_3 and AlN showed recovery from 400 ℃, while an interstitial atom is considered to have enough mobility to recombine with a vacancy at 100 ℃. The distribution of defects is discussed, but it could not explain this difference. Further investigation of the annealing behavior of the electron-irradiated specimen is required to accurately determine the temperature of the specimen during irradiation using an analysis based on reaction kinetics.

References

[1] Akiyoshi M., Tsuchida H., Yano T., Thermal diffusivity of ceramics during neutron irradiation, In: "Advances in Ceramics - Characterization, Raw Materials, Processing, Properties, Degradation and Healing", ed. C. Sikalidis, InTech 2011; p.39–58.

[2] Snead L.L., Nozawa T., Katoh Y., Byun T., Kondo S., Petti D.A., Handbook of SiC properties for fuel performance modeling, J. Nucl. Mater. 2007;371:329–377.

[3] Akiyoshi M., Thermal diffusivity of ceramics at the neutron irradiation temperature estimated from post-irradiation measurements at 123-413 K, J. Nucl. Mater. 2009;386-388:303–306.

[4] Akiyoshi M., Takagi I., Yano T., Akasaka N., Tachi Y., Thermal conductivity of ceramics during irradiation, Fusion Eng. Design 2006;81:321–325.

[5] Tsuchida H., Iwai T., Kasai S., Tanaka H., Oshima N., Suzuki R., T. Yoshiie, Itoh A., Vacancy evolution in Ni during irradiation at high temperatures studied by in situ positron annihilation spectroscopy, J. Phys.: Conference Series 2011;262:012060.

[6] Tsuchida H., Iwai T., Awano M., Kishida M., Katayama I., Jeong SC., Ogawa H., Sakamoto N., Komatsu M., Itoh A., Observation of transient lattice vacancies produced during high-energy ion irradiation of Ni foils, J. Phys. Condens. Matter 2007;19:136205.

[7] Iwai T., Ito Y., Koshimizu M., Vacancy-type defect production in iron under ion beam irradiation investigated with positron beam Doppler broadening technique, J. Nucl. Mater. 2004;329-333 Part2:963–966.

[8] Ryazanov A., Yasuda K., Kinoshita C., Klaptsov A., Instability of interstitial clusters under ion and electron irradiations in ceramic materials, J. Nucl. Mater. 2003;323:372–379.

[9] Kinoshita C., Zinkle S., Potential and limitations of ceramics in terms of structural and electrical integrity in fusion environments, J. Nucl. Mater. 1996;233-237:100–110.

[10] Howlader M., Kinoshita C., Izu T., Shiiyama K., Kutsuwada M., In situ measurement of electrical conductivity of alumina under electron irradiation in a high voltage electron microscope, J. Nucl. Mater. 1996;239:245–252.

[11] Shikama T., Pells G., A comparison of the effects of neutron and other irradiation sources on the dynamic property changes of ceramic insulators, J. Nucl. Mater. 1994;212-215:80–89.

[12] Moritani K., Takemoto J., Takagi I., Akiyoshi M., Moriyama H., Reaction kinetics of radiation-induced defects in vitreous silica under ion beam irradiation, J. Nucl. Mater. 2009;384:19–24.

[13] Moritani K., Teraoka Y., Takagi I., Akiyoshi M., Moriyama H., Production and reaction kinetics of radiation-induced defects in alpha-alumina and sapphire under ion beam irradiation, J. Nucl. Mater. 2008;373:157–163.

[14] Akiyoshi M., Yano T., Neutron-irradiation effect in ceramics evaluated from macroscopic property changes in as-irradiated and annealed specimens, Prog. Nucl. Energy 2008;50:567–574.

[15] Akiyoshi M., Akasaka N., Tachi Y., Yano T., Interstitial atom behavior in neutron-irradiated beta-silicon nitride, J. Ceram. Soc. J. 2004;112:1490–1494.

[16] Akiyoshi M., Ichikawa K., Donomae T., Yano T., Macroscopic properties and microstructure changes of heavily neutron-irradiated β-Si_3N_4 by annealing, J. Nucl. Mater. 2002;307-311:1305–1309.

[17] Yano T., Akiyoshi M., Ichikawa K., Tachi Y., Iseki Y., Physical property change of heavily-neutron-irradiated Si_3N_4 and SiC by thermal annealing, J. Nucl. Mater. 2001;289:102–109.

[18] Yano T., Ichikawa K., Akiyoshi M., Tachi Y., Neutron irradiation damage in aluminum oxide and nitride ceramics up to a fluence of 4.2×10^{26}n/m^2, J. Nucl. Mater. 2000;283-287:947–951.

[19] Akiyoshi M., Yano T., Jenkins M., A structural model of defects in β-Si_3N_4 produced by neutron-irradiation, Phil. Mag. A 2001;81:683–697.

[20] Akiyoshi M., Yano T., Tachi Y., Nakano H., Saturation in degradation of thermal diffusivity of neutron-irradiated ceramics at 3×10^{26}n/m^2, J. Nucl. Mater. 2007;367-370:1023–1027.

[21] Hickman B.S., Walker D.G., The effect of neutron irradiation on aluminium oxide, J. Nucl. Mater. 1966;18:197–205.

[22] Rohde M., Schulz B., The effect of the exposure to different irradiation sources on the thermal conductivity of Al_2O_3, J. Nucl. Mater. 1990;173:289–293.

[23] Wilks. R.S., Neutron-induced damage in BeO, Al_2O_3 and MgO – A review, J. Nucl. Mater. 1968;26:186.

[24] Wilks R.S., Desport J., Smith J., The irradiation-induced macroscopic grpwth of α-Al_2O_3 single crystals, J. Nucl. Mater. 1967;24:80–86.

[25] Clinard Jr. F.W., Dienst W., Farnum E.H., Issues related to mechanical properties of neutron-irradiated ceramics, J. Nucl. Mater. 1994;212-215:1075–1080.

[26] Clinard Jr. F.W., Hurley G.F., Hobbs L.W., Neutron irradiation damage in MgO, Al_2O_3 and $MgAl_2O_4$ ceramics, J. Nucl. Mater. 1982;108-109:655–670.

[27] Yano T., Miyazaki H., Iseki T., Effect of isochronal annealing on thermal diffusivity of neutron-irradiated AlN, J. Nucl. Mater. 1996;230:74–77.

[28] Suematsu H., Mitchell T., Iseki T., Yano T., Hardening in AlN induced by point defects, Mater. Res. Soc. Sympo. Proc. 1992;235:445–450.

[29] Yano T., Tezuka M., Miyazaki H., Iseki T., Macroscopic length, lattice parameter and microstructural change in neutron-irradiated aluminium nitride due to annealing, J. Nucl. Mater. 1992;191-194:635–639.

[30] Yano T., Miyazaki H., Akiyoshi M., Iseki T., X-ray diffractometry and high-resolution electron microscopy of neutron-irradiated SiC to a fluence of 1.9×10^{27} n/m^2, J. Nucl. Mater. 1998;253:78–86.

[31] Miyazaki H., Suzuki T., Yano T., Iseki T., Effect of thermal annealing on the macroscopic dimension and lattice parameter of heavily neutron-irradiated silicon carbide, J. Nucl. Science and Technol. 1992;29:656–663.

[32] Suzuki T., Yano T., Maruyama T., Iseki T., Effect of sintering aids on the length change of neutron irradiated SiC ceramics during annealing at high temperature, J. Nucl. Mater. 1989;165:247–251.

[33] Yano T., Sasaki K., Maruyama T., Iseki T., Ito M., Onose S., A step-heating dilatometry method to measure the change in length due to annealing of a SiC temperature monitor, Nucl. Technol. 1991;93:412–415.

[34] Akiyoshi M., Akasaka N., Tachi Y., Yano T., Relation between macroscopic length change and the crystal structure in heavily neutron-irradiated ceramics, J. Nucl. Mater. 2004;329-333:1466–1470.

[35] Bullough R., Newman R.C., The kinetics of migration of point defects to dislocations, Reports on Prog. in Phys. 1970;33:101.

[36] Clinard Jr. F.W., Hobbs L.W., Physics of Radiation Effects in Crystals, ed. Johonson R.A. and Orlov A.N., Elsevier 1986; Vol. 13: p.387,